magPEEC: Extended PEEC Modeling for 3D Arbitrary Electro-Magnetic Devices with Application for M-Cored Inductors

Haibo Long[1], Zhenghe Feng[1], Haigang Feng[2], Albert Wang[2] and Tianling Ren[3]

[1] State Key Lab on Microwave and Digital Communications, Dept. EE, Tsinghua University, Beijing, 100084, China. Phone: (8610)62781453; Fax: (8610)62770317; Email: fzh-dee@mail.tsinghu.edu.cn

[2] Integrated Electronics Laboratory, Dept. ECE, Illinois Institute of Technology, Chicago, IL 60616, USA. Phone: 312-567-6912; Fax: 312-567-8976; Email: awang@ece.iit.edu

[3] Institute of Microelectronics, Tsinghua University, Beijing, 100084, China

Abstract — This paper presents magPEEC, a new 3D electro-magnetic modeling technique that extends existing PEEC approach to analyze arbitrary conductor-magnet structures by accounting for fictitious magnetized currents on magnetic material surface. Applications of magPEEC for magnetic-cored RF IC inductors are discussed with examples of stacked spiral inductors in 0.18μm CMOS. The observed upper-limit effect of enhancing inductance by increasing magnetic permeability is also discussed.

I. Introduction

Nowadays, magnetic materials have been widely used to make electro-magnetic (EM) structures such as MEMS (Micro Electro Mechanical Systems) and on-chip spiral inductors for RF IC applications to improve inductances and quality factors. Inductors using magnetic films operated at multi-GHz frequency have been reported [1]. Existing full-wave approaches such as finite difference or finite element method are unsuitable for analyzing these structures with magnetic films or cores because the complex meshes and large number of unknowns make such simulation impractical due to its computational deficiency. The simulation approaches given in [2] and [3] have limited applications due to their 2D nature. [4] reported a new simulation program called Fastmag, which can only deal with structures with magnetic materials separated from electrical conductors and is not suitable for true 3D structure simulation due to the equivalent loop structure mesh cell used. Partial element equivalent circuit (PEEC) approach was firstly proposed to model 3D multi-conductor systems in [5], which was later extended to include electrical dielectrics [6]. This paper presents a new modeling technique, entitled magPEEC, which extends the PEEC approach to analyze arbitrary 3D electro-magnetic structures that permits conductors to be outside, contacting or inside magnetic materials – a desired feature for modeling many sophisticated electro-magnetic structures.

II. magPEEC: Magnetic Materials Included

For arbitrary 3D EM structure with conductors and magnetic materials, currents are distributed in three fields: region α denoting conductor bodies outside magnetic materials, regions β and γ denoting magnetic surfaces with and without contacting conductors, respectively. By using fictitious magnetized currents on magnetic material surface, the calculation is equivalent to the free space problem. The real conductive current density and fictitious magnetized current density at a point $\bar{r}$ are denoted as $\bar{J}_c(\bar{r})$ and $\bar{J}_f(\bar{r})$, respectively. The total equivalent current density denoted as $\bar{J}_t(r)$ is based on $\bar{J}_t(\bar{r}) = \bar{J}_c(\bar{r}) + \bar{J}_f(\bar{r})$. The corresponding currents through a mesh cell are denoted as I_c, I_f and I_t, respectively.

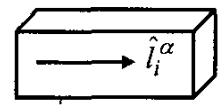

Fig. 1. A filament cell of region α.

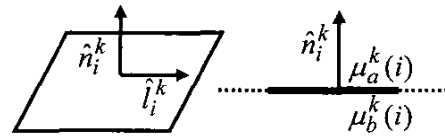

Fig. 2. A panel cell of region k ($k = \beta, \gamma$).

Region α is discretized into N^{α} filament cells (carrying bulk currents) as shown in Fig.1. Related parameters for the i^{th} filament cell include current flowing direction $\hat{l}_i^{\alpha}$, through electrical voltage V_i^{α}, bulk v_i^{α}, current crossing area a_i^{α} and current flowing length L_i^{α}. Region β and γ are discretized into N^{β} and N^{γ} panel cells (carrying surface currents),

0-7803-7694-3/03/$17.00 © 2003 IEEE

respectively, as shown in Fig.2. Related parameters for the i^{th} panel cell in region β or γ include current flowing direction $\hat{l}_i^k$, through electrical voltage V_i^k, area s_i^k, current crossing width W_i^k, current flowing length L_i^k, the panel's normal direction $\hat{n}_i^k$. $\mu_a^k(i)$ and $\mu_b^k(i)$ are permeabilities of a and b sides. $\mu_{ra}^k(i)$ and $\mu_{rb}^k(i)$ are corresponding relative permeabilities. The current density over each of these cells is assumed locally constant.

Analogous to problems in free space, magnetic vector potential is obtained as:

$$\bar{A} = \frac{\mu_0}{4\pi}\sum_{j=1}^{N^\alpha}\frac{I_{ij}^\alpha \hat{l}_j^a}{a_j^\alpha}\int_{(v_j^\alpha)'}\frac{1}{|\bar{R}|}dv' + \frac{\mu_0}{4\pi}\sum_{j=1}^{N^\beta}\frac{I_{ij}^\beta \hat{l}_j^\beta}{W_j^\beta}\int_{(s_j^\beta)'}\frac{1}{|\bar{R}|}ds' + \frac{\mu_0}{4\pi}\sum_{j=1}^{N^\gamma}\frac{I_{ij}^\gamma \hat{l}_j^\gamma}{W_j^\gamma}\int_{(s_j^\gamma)'}\frac{1}{|\bar{R}|}ds' \quad (1)$$

where $\bar{R} = \bar{r} - \bar{r}'$, $\bar{r}$ is field point and $\bar{r}'$ is source point. Magnetic flux density is extracted by $\bar{B} = \nabla \times \bar{A}$. Based on PEEC approach [5] by considering currents and voltages of each cell in region α and β, we obtain

$$\left[V^\alpha\right] = \left[Z^{\alpha\alpha}\right]\left[I_i^\alpha\right] + \left[Z^{\alpha\beta}\right]\left[I_i^\beta\right] + \left[Z^{\alpha\gamma}\right]\left[I_i^\gamma\right] \quad (2)$$

$$\left[V^\beta\right] = \left[Z^{\beta\alpha}\right]\left[I_i^\alpha\right] + \left[Z^{\beta\beta}\right]\left[I_i^\beta\right] + \left[Z^{\beta\gamma}\right]\left[I_i^\gamma\right] \quad (3)$$

where $\left[Z^{kh}\right](k = \alpha,\beta; h = \alpha,\beta,\gamma)$ are impedance matrixes with the element $Z_{mn}^{kh} = j\omega L_{mn}^{kh} + \delta_{kh}\delta_{mn}R_m^k$. L_{mn}^{kh} is partial inductance of the m^{th} cell in region k due to the n^{th} cell in region h. R_m^k is partial resistance of the m^{th} cell in region k and δ_{mn} is Kroniker delta function. Extracting the real conductive current flowing through each panel cell in region β or γ with constant conductive current density $\bar{J}_{ci}^k$ ($k = \beta,\gamma$), we obtain

$$I_{ci}^k = W_i^k(\hat{l}_i^k \cdot \bar{J}_{ci}^k) = W_i^k(\hat{l}_i^k \cdot \frac{1}{s_i^k}\int_{s_i^k}\bar{J}_{ci}^k ds) \quad (4)$$

and the magnetic border condition is,

$$\bar{J}_c = \hat{n} \times (\frac{\bar{B}(\bar{r}_a)}{\mu_a} - \frac{\bar{B}(\bar{r}_b)}{\mu_b}) \quad (5)$$

here $\bar{r}_a$ and $\bar{r}_b$ approach the border from a and b sides. Substitute Eq (5) into Eq (4), we obtain Eqs (6) & (7),

$$\left[I_c^\beta\right] = \left[F^{\beta\alpha}\right]\left[I_i^\alpha\right] + \left[F^{\beta\beta}\right]\left[I_i^\beta\right] + \left[F^{\beta\gamma}\right]\left[I_i^\gamma\right] \quad (6)$$

$$\left[I_c^\gamma\right] = \left[F^{\gamma\alpha}\right]\left[I_i^\alpha\right] + \left[F^{\gamma\beta}\right]\left[I_i^\beta\right] + \left[F^{\gamma\gamma}\right]\left[I_i^\gamma\right] \quad (7)$$

where the matrix element F_{mn}^{kh} ($k = \beta,\gamma; h = \alpha,\beta,\gamma$) represents the coupling effect of I_{cm}^k due to I_{in}^h. Although the derivation of F_{mn}^{kh} is cumbersome, we got a fairly simple expression as Eq (8) where the term GF is the geometry factor which is composed of four- or five-fold integrals over hexahedrons or quadrangles, which may be computed by using existing fast and accurate techniques. Magnetic materials with relative permeability of infinity can be simulated by neglecting the reciprocal term of infinity in Eq (8).

$$F_{mn}^{kh} = \begin{cases} \frac{1}{2}(\frac{1}{\mu_{ra}^k(m)} + \frac{1}{\mu_{rb}^k(m)}) & (k = h \ \& \ m = n) \\ \frac{1}{2}(\frac{1}{\mu_{ra}^k(m)} - \frac{1}{\mu_{rb}^k(m)}) \times GF & (else) \end{cases} \quad (8)$$

The following equations are obtained readily,

$$\left[I_i^\alpha\right] = \left[I_c^\alpha\right] \quad (9)$$

$$\left[I_c^\gamma\right] = [0] \quad (10)$$

Substituting Eq (9) into Eqs (2-3) & (6-7) and plugging Eq (10) into Eq (7), then eliminating I_i^β and I_i^γ from Eqs (2) & (3) by using Eqs (6) & (7), we can get the relation between through voltages and conductive currents of cells in region α & β as follows,

$$\begin{bmatrix} V^\alpha \\ V^\beta \end{bmatrix} = \left[Z^L\right]\begin{bmatrix} I_c^\alpha \\ I_c^\beta \end{bmatrix} \quad (11)$$

In PEEC, the matrix $\left[Z^L\right]$ is called inductance matrix. Here the inductance matrix has been extended to include magnetic material effects.

III. Applications For Stacked Spiral Inductors With Magnetic Cores

The new magPEEC technique was used to develop a new CAD tool, entitled L-Simulator, which can accurately simulate magnetic-cored/covered RF IC inductors. To verify the validity and accuracy of the magPEEC modeling technique and the L-Simulator software, L-Simulator was used to simulate several different on-chip inductors from publications and our own designs. Generally, for spiral inductors with magnetic layer underneath or with magnetic cores (M-cored) inside, all currents-carrying metal stripes are outside magnetic materials. Hence, the problem is simplified to dealing with regions α & γ. The simulation procedures follow: Metal stripes are first divided into K segments. Each segment is then discretized into a number of filament cells to simulate both skin effects and proximity effects in conductors as described in [7]. The total number of filament cells is N^α. Finally, magnetic surfaces are discretized into N^γ panel cells. The inductance matrix is

solved using the magPEEC approach. Inductance L_s and resistance R_s of the structure can be extracted by using the technique given in [8].

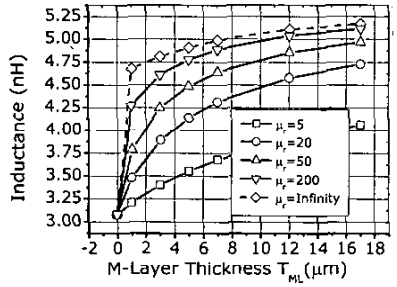

Fig. 3. Simulation data for multi-layer spiral inductors with magnetic layer underneath

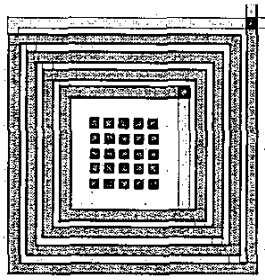

Fig. 4. A cross-section of a novel spiral inductor with stacked-via magnetic core arrays in CMOS [10].

In the first example, we simulated a conventional planner spiral inductor similar to those magnetic structures reported in [2-4]. The basic structure is a 4-turn square spiral inductor of [9] with metal width of 10μm, spacing of 2μm and inner diameter of 100μm. To validate our model and confirm the observations of [2-4], magnetic films with varying thickness were positioned 3μm lower underneath metal coil. Simulation results confirmed that significant improvement in inductances and quality factors due to the magnetic films used. Further, Fig. 3 clearly shows that while the inductance continuously improve as the permeability value increases, this improvement saturates and reaches to an upper limit, with its peak value less than the possible maximal peak value which is almost doubling the value of the same inductor without magnetic layer, which confirms the similar observations reported in [2-4]. In addition, the simulated inductance without magnetic film of about 3.0nH and its resistance of 7.70 Ω agree well with the measured values 2.85nH and 7.87 Ω, respectively, reported in [9].

As the second example, we simulated several true-3D inductors we designed and fabricated in a commercial 0.18μm, 6-metal, all copper CMOS technology [10]. The first one is a super compact 22μm x 23μm, six-layer stacked spiral inductor as shown in Fig. 4 for its cored version, featuring four turns per spiral, 1μm metal line width and 0.5μm metal line spacing. The measured inductance and resistance are 9.52nH and 98.1 Ω, respectively, for the inductor, which agrees well with the simulated 9.44nH and 99.50 Ω as shown in Fig.5. Aiming to design transistor-sized super compact RF IC inductors with improved inductance and quality factor, we proposed a novel stacked-via magnetic-cored inductor structure for standard CMOS technologies. The fabrication of these novel stacked-via-cored inductors is currently underway. Fig. 4 shows the similar structure fabricated in the 0.18μm CMOS with dummy magnetic cores for feasibility study. The magPEEC-based L-Simulator was used to predict the performance of this novel design before running silicon.

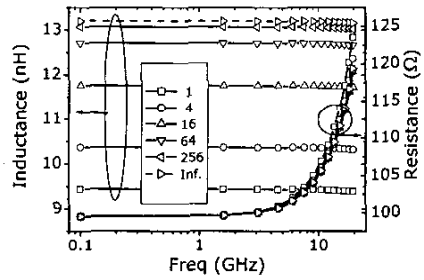

Fig. 5. Simulation results for the array-M-cored inductors with various relative permeability values marked with legends.

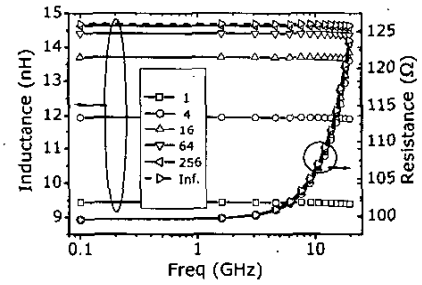

Fig. 6. Simulation results for the single-magnetic-cored inductor with various relative permeability values marked with legends.

For comparison purpose, two layout versions were designed with the first one featuring a stacked-via core

array of 25 cores (core thickness H_{MC} of 7μm, core diameter D_{MC} of 1.12μm and core spacing SP_{MC} of 1.6μm) and the second having a single core of D_{MC} = 12μm. The inductor metal structures are same as the uncored one described above. Fig.5 and Fig.6 show the simulated data for the two style M-cored inductors. Firstly, the data show that inductance improvement due to magnetic cores saturates as the permeability increases to some threshold value (i.e., 100+ in this case). Secondly, inductance of structure with core array is lower than that with single core, most likely due to the fact that the effective magnetic fluxing area of the array-cored structure is less than that of single-cored inductor, given everything else being the same. However, this may not be the general case because a big single-cored structure may result in current crowding in lossy magnetic material cases. The array-cored structure may be a better choice in lifting up the upper limit of the inductance~permeability relationship observed by minimizing the core spacing, SP_{MC}. Thirdly, the observation that the inductance~permeability improvement saturates as permeability approaches to 100+ suggests that one might not have to struggle to find the super-permeability magnetic materials for making super cored inductors. Instead, layout design shall optimize inductor performance. Fourthly, the data suggest that the parasitic resistance is insensitive to the lossy nature of the magnetic materials used in array-cored inductors.

The root cause of the observed upper-limit effect in the inductance-permeability relationship is subjected to further investigation. Simulation data in Figs 5 & 6 suggests that this relationship can be divided into three segments corresponding to relative permeability from 1 to infinity, i.e., linear, transitional and saturated regions. In the desired linear region, inductance improvement due to M-materials is proportional to the permeability. In the to-be-avoided saturated region, no inductance improvement is expected. Unfortunately, Figs 5 & 6 show that the desired linear relationship virtually does not exist for M-cored IC inductors, where improvement of M-cored IC inductors might only be expected in the transitional region. This observation suggests that the right approach of designing good M-cored IC inductors is to optimize the structure to expand the transitional region into linear region and to select suitable magnets of high permeability and low Ohmic loss.

IV. Conclusion

We present a new 3D electro-magnetic modeling technique, called magPEEC, which extends existing PEEC approach to analyze arbitrary conductor-magnet structures by accounting for fictitious magnetic currents on magnetic material surface. The magPEEC approach was used to develop a magnetic-core inductor simulator, L-Simulator, which can also be used to simulate other types of electro-magnetic structures of arbitrary 3D geometries. Example RF IC inductors designed in 0.18μm CMOS technology are given to demonstrate the validity and accuracy of the magPEEC and the simulator developed. Excellent agreements between simulation and measurements were achieved. Design prediction using magPEEC-based simulator was discussed for M-cored RF IC inductors. Observation of the upper-limit effect in inductance-permeability relationship is discussed.

V. Acknowledgement

This paper is supported by National "973" R&D Project of China (NO. G1999033105) and National Natural Science Foundation of China (NO. 60171015)

Reference

[1] M. Yamaguchi, et al, "Sandwich-type ferromagnetic RF integrated inductor", *IEEE Trans. Microwave Theory and Tech.*, vol. MTT-49, no. 12, pp. 2331-2335, Dec. 2001.

[2] W. A. Roshen, "Effect of finite thickness of magnetic substrate on planar inductors", *IEEE Trans. Magnetics*, vol. 26, no. 1, pp. 270-275, Jan. 1990.

[3] S. F. Mahnoud, et al, "Inductance and quality-factor evaluation of planar lumped inductors in a multilayer configuration", *IEEE Trans. Microwave Theory and Tech.*, vol. MTT-45, no. 6, pp. 918-923, June 1997.

[4] Y. Massoud, et al, "FastMag: a 3-D magnetostatic inductance extraction program for structures with permeable materials", *in Proc. of International Conference on Computer Aided Design*, vol. 1, pp. 478-484, Nov. 2002.

[5] A. E. Ruehli, "Equivalent circuit models for three-dimensional multiconductor systems", *IEEE Trans. Microwave Theory and Tech.*, vol. MTT-22, no.3, pp. 216-221, Mar. 1974.

[6] A. E. Ruehli, et al, "Circuit models for three-dimensional geometries including dielectrics", *IEEE Trans. Microwave Theory and Tech.*, vol. MTT-40, no. 7, pp. 1507-1516, July 1992.

[7] W. T. Weeks, "Resistive and inductive skin effect in rectangular conductors", *IBM J. RES. DEVELOP.*, vol. 23, no. 6, pp. 652-660, Nov. 1979.

[8] Y. J. Zhang, et al, "Analysis of current-crowding effects in RF-MEMS spiral inductors by simple equivalent circuits", *Microwave and Optical Technology Letters*, vol. 33, no. 3, pp. 218-221, May 2002.

[9] M. Park, et al, "The detailed analysis of high Q CMOS-compatible microwave spiral inductors in silicon technology", *IEEE Trans. Electron Devices*, vol. 45, no. 9, pp.1953-1959, Sep. 1998.

[10] H. Feng, et al, "Super compact RFIC Inductors in 0.18 *μm* CMOS with Copper Interconnects", *2002 IEEE MTT-S Int. Microwave Symp. Dig.*, vol. 1, pp. 553-556, June 2002.